Proc. Schl. Eng. Tokai Univ., Ser. E
36 (2011) 21-28

Vibroacoustic Coupling of a Cylindrical Enclosure with an Excited End Plate

by

Atsushi KOJIMA*1, Hiroyuki MORIYAMA*2 and Yasuo OSHINOYA*2

(Received on Apr. 14, 2011 and accepted on Jun. 08, 2011)

Abstract

Being extremely minute in comparison with other sources of industrial energy, acoustic energy must be amplified for use in industrial applications. In the present study, we consider a cylindrical structure with thin plates at both ends and investigate vibroacoustic coupling between the plate vibrations and the internal sound field when an external harmonic force is applied to one end plate, regarding such a coupling phenomenon as one of the available measures to amplify acoustic energy. This coupling is investigated theoretically and experimentally by considering the behavior of both plates and the acoustic characteristics of the internal sound field for various dimensions of the end plates and the cylinder. In the analytical model, the end plates are supported circumferentially by springs so that the support conditions can be made to closely match the actual conditions in the experiment by adjusting the stiffnesses of the springs. Then, in order to simplify this problem, the cylinder is assumed to be structurally and acoustically rigid at the lateral wall between the structure and the sound field. The dimensions and phase differences between plate vibrations, which maximize the sound pressure level inside the cavity, are clarified theoretically. These theoretical results are verified experimentally through an excitation experiment using an experimental apparatus that is emulated by the analytical model. The above-described results reveal that vibroacoustic coupling phenomena are useful for the amplification of the acoustic energy.

Keywords: Vibroacoustic Coupling, Cylindrical Enclosure, Structural Vibration, Internal Sound Field

1. Introduction

Although we are constantly surrounded by vibrations and sounds, most of these dissipate into the environment and are not used as sources of industrial energy. In particular, acoustic energy is extremely minute in comparison with vibration energy, and so applications of acoustic energy in mechanical engineering have been limited. However, in order to promote energy savings and suppress the greenhouse effect, the application of acoustic energy, e.g., sound-generated electricity from a voice obtained via piezoelectric elements installed on elastic plates, is regarded as advantageous. Although this electric generation system was developed as a supplementary electricity source for a mobile phone[1)], this system is being investigated for application in other devices[2)]. Since the electricity is generated by both sound and vibration systems, vibroacoustic coupling between both systems is one means of amplifying the acoustic energy. However vibroacoustic coupling is not used in the above-mentioned example.

In order to develop a new electricity generation system, we adopt an analytical model similar to the above-mentioned cylindrical structure with plates at both ends, because the vibration area of the model, on which piezoelectric elements can be installed, is twice as large as that in the case of a single plate. In almost all related studies, vibroacoustic coupling was estimated by assuming that the plate and cavity dimensions and the phase difference between the vibrations of the two plates were fixed. However, the eigenfrequencies of the plate and cavity vary with the dimensions of the plate and cavity, and the phase difference directly affects the sound field when the medium is much less dense than the plate. Accordingly, in this investigation, the dimensions of both the plate and the cylinder are varied over a wide range while a harmonic point force is applied to only one end plate. Vibroacoustic coupling that occurs between plate vibrations and the sound field in the cavity is theoretically and

*1 Graduate Student, Course of Science and Technology
*2 Professor, Department of Prime Mover Engineering

experimentally investigated in terms of the vibration and acoustic characteristics. In particular, the phase difference between the vibrations of the two plates is considered to be a significant characteristic of the vibrations, and the conditions for maximizing the sound pressure level in the cavity is clarified in order to apply the coupling phenomena to the new generation system.

2. Analytical method

2.1 *Analytical model*

The analytical model considered herein consists of a cavity with two circular end plates, as shown in Fig. 1. The plates are supported by translational and rotational springs distributed at constant intervals and the support conditions are determined by their respective spring stiffnesses, T_1 and T_2, and R_1 and R_2, where the suffixes 1 and 2 indicate plates 1 and 2, respectively. The dimensions (i.e., the radius a and the thickness h) of the plates, which have Young's modulus E and Poisson's ratio ν, are varied. The sound field is assumed to be cylindrical and to have the same radius as the plates, and the length of the sound field is assumed to vary with the cylinder length. The boundary conditions are considered to be structurally and acoustically rigid at the lateral wall between the structure and the sound field. The coordinates used are the radius r, the angle θ between the planes of the plates and the cross-sectional plane of the cavity, and the distance z along the cylinder axis. The harmonic point force F_1 is applied to plate 1 at r_1 divided by a, and θ_1 is fixed at 0 deg. The natural frequency of the plate is used as its excitation frequency.

2.2 *Coupling equipment between plates and cavity*

In order to formulate the plate motion, Hamilton's principle based on the variational principle is applied to the analytical model[3] and the flexural displacements w_1 and w_2 on plates 1 and 2 are expressed by substituting Eq. (2) for the plate mode shape into Eq. (1) and are expanded over two sets of suitable trial functions:

$$\left.\begin{aligned} w_1 &= \sum_{s=0}^{1}\sum_{n=0}^{\infty}\sum_{m=0}^{\infty} B^s_{1nm} X^s_{nm} \mathrm{e}^{\mathrm{j}(\omega t+\phi_1)}, \\ w_2 &= \sum_{s=0}^{1}\sum_{n=0}^{\infty}\sum_{m=0}^{\infty} B^s_{2nm} X^s_{nm} \mathrm{e}^{\mathrm{j}(\omega t+\phi_2)}, \end{aligned}\right\} \quad (1)$$

$$X^s_{nm} = \sin(n\theta + s\pi/2)(r/a)^m, \quad (2)$$

where n, m, and s are, respectively, the circumferential order, the radial order, and the symmetry index for the z-axis of the vibration mode with respect to the plate vibration. In addition, $B^s{}_{1nm}$ and $B^s{}_{2nm}$ are the coefficients to be determined, ω is the angular frequency of the harmonic point force on the plate, t is the elapsed time, and ϕ_1 and ϕ_2 are the phases of the respective plate vibrations. In this analysis, ϕ_1 is set to 0 deg, and ϕ_2 varies in the range of 0 to 180 deg. The equations of plate motion are obtained by finding the extremum of Hmilton's function in terms of Eqs. (1).

The acoustic modal shape $Y^s{}_{npq}$ and angular resonance frequency ω_{npq} in the cavity (where the indexes n, p, and q indicate the circumferential, radial, and longitudinal orders, respectively) are defined as

$$Y^s_{npq} = \sin(n\theta + s\pi/2) J_n(\lambda_{np} r)\cos\{(q\pi/L)z\}, \quad (3)$$

$$\omega_{npq} = c\left\{\lambda_{np}{}^2 + (q\pi/L)^2\right\}^{1/2}, \quad (4)$$

where J_n is the nth-order Bessel function, and λ_{np} is the p-th solution of an eigenvalue function for a circular sound field having (n,p) modes divided by the radius. The boundary conditions between the plate vibrations and the sound field on the respective plate surfaces are found by assuming continuity of velocities on the plates:

$$\left(\frac{\partial P_c}{\partial \mathbf{u}}\right)_{z=0} = \rho_c \omega^2 w_1 \quad , \quad \left(\frac{\partial P_c}{\partial \mathbf{u}}\right)_{z=L} = -\rho_c \omega^2 w_2, \quad (5)$$

where P_c and ρ_c are, respectivery, the sound pressure on each boundary surface (e.i., each plate surface) and the fluid density in the cavity, and $\mathbf{u}$ is the unit normal to the corresponding plate surfaces, such that $\partial Pc\ /\partial \mathbf{u}$ is 0 on the lateral wall of the cylinder. Moreover, in the present analysis we assume that there is no sound source, and hence by using the above boundary conditions and Green's function for a non-uniform cavity with non-rigid walls, P_c can be expanded in terms of the acoustic modes consisting of a trio of orders, n, p and q, as follows:

$$P_c = -\int_{A_1} G\rho_c\omega^2 w_1 \mathrm{d}A_1 + \int_{A_2} G\rho_c\omega^2 w_2 \mathrm{d}A_2 = \rho_c c^2 \sum_{p=1}^{\infty}\sum_{q=0}^{\infty} \frac{P^s_{npq} Y^s_{npq}}{M^s_{npq}} \quad (6)$$

where G is Green's function, A is the total surface area of the plates, and $P^s{}_{npq}$ and $M^s{}_{npq}$ are, respectively, the pressure coefficients to be determined and the modal generalized mass of the nth acoustic modes.

When one end plate excited by point force is coupled by a cavity, the coupling equations between the plate vibtrations and the sound field are expressed as [4,5]

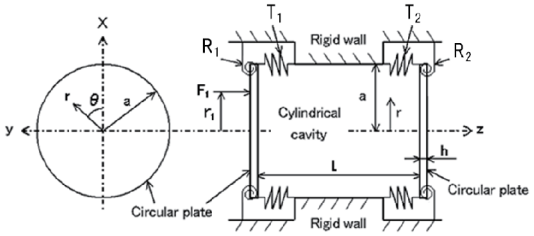

Fig. 1 Configuration of the analytical model

$$\left[\sum_{m'=0}^{\infty}\left\{K^s_{1nmm'}\left(1+\mathrm{j}\eta_p\right)-\omega^2 M^s_{1nmm'}\right\}+\sum_{m'=0}^{\infty}aF_{sn}\left\{T_1+\left(\frac{m}{a}\right)\left(\frac{m'}{a}\right)R_1\right\}\right]\mathbf{B}^s_{1nm'}\mathrm{e}^{\mathrm{j}\phi_1}$$
$$=\mathbf{F}^s_{1nm}+\frac{\rho_c c^2\omega^2 A^2}{V_c}\sum_{m'=0}^{\infty}\sum_{p=1}^{\infty}\sum_{q=0}^{\infty}\frac{I_1\left(I_1B^s_{1nm'}\mathrm{e}^{j\phi_1}-I_2B^s_{2nm'}\mathrm{e}^{j\phi_2}\right)}{M^s_{npq}\left(\omega^2_{npq}+\mathrm{j}\eta_c\omega_{npq}\omega-\omega^2\right)}, \tag{7}$$

$$\left[\sum_{m'=0}^{\infty}\left\{K^s_{2nmm'}\left(1+\mathrm{j}\eta_p\right)-\omega^2 M^s_{2nmm'}\right\}+\sum_{m'=0}^{\infty}aF_{sn}\left\{T_2+\left(\frac{m}{a}\right)\left(\frac{m'}{a}\right)R_2\right\}\right]\mathbf{B}^s_{2nm'}\mathrm{e}^{\mathrm{j}\phi_2}$$
$$=-\frac{\rho_c c^2\omega^2 A^2}{V_c}\sum_{m'=0}^{\infty}\sum_{p=1}^{\infty}\sum_{q=0}^{\infty}\frac{I_2\left(I_1B^s_{1nm'}\mathrm{e}^{j\phi_1}-I_2B^s_{2nm'}\mathrm{e}^{j\phi_2}\right)}{M^s_{npq}\left(\omega^2_{npq}+\mathrm{j}\eta_c\omega_{npq}\omega-\omega^2\right)}, \tag{8}$$

where $K^s{}_{1nmm'}$ and $K^s{}_{2nmm'}$, and $M^s{}_{1nmm'}$ and $M^s{}_{2nmm'}$ are components of the symmetrical stiffness and mass matrices, respectively, because the index m' is the radial order ($m = m$'). In addition, η_p is the structural damping factor of the plate, and F_{sn} is a coefficient that is determined by indices n and s[3]. On the right-hand side of Eq. (7), the first and second terms express the point force and coupling between each plate vibration and the sound field, respectively, whereas the right-hand side of Eq. (8) contains only the coupling term. Here, c is the speed of sound in the cavity, and V_c is the volume occupied by the cavity. Moreover, I_1 and I_2 are, respectively, the spatial coupling coefficients between the end plates and cavity, and η_c is the acoustical damping factor inside the cavity. Furthermore, since $B^s{}_{1nm'}$ and $B^s{}_{2nm'}$ can be obtained from the above equations, the behaviors of plate vibrations and the sound field under vibroacoustic coupling can be determined.

3. Theoretical results and discussion

3.1 *Effect of plate vibrations on acoustic characteristics*

In the present study, the plates are assumed to be aluminum having a Young's modulus E of 71 GPa and a Poisson's ratio ν of 0.33. Most of the plates have a radius a of 100, 150 or 200 mm and a thickness h of 3 mm. All combinations of these dimensions are considered in the analysis, however complementary dimensions are also used in the parametric study. The length of the cylindrical sound field having the same radius as the plates varies in length from 100 to 2000 mm. The support conditions of the plates, which have flexural rigidity D [$= Eh^3/\{12(1-\nu^2)\}$], are expressed by the non-dimensional stiffness parameters T_n ($= T_1a^3/D = T_2a^3/D$) and R_n ($= R_1a/D = R_2a/D$). In the present study, these values are identical for both plates. Here, R_n ranges from 0 to 10^8 when T_n is 10^8, and hence the support condition varies from a simple support to a clamped support. The natural frequency of the plate corresponding to the (n,m) mode is expressed as f_{nm} and is regarded as the excitation frequency. This natural frequency depends both on the support conditions and the vibration mode. When the (0,0), (1,0), and (0,1) modes are taken into consideration and the excitation position moves radially to a location near the nodal line or circle of the plate vibration, the excitation position also affects the plate vibration characteristics, the internal sound field, and the coupling between the respective vibrations and the sound field. The (1,0) mode has a nodal line on the radius, so that the excitation position is set as $r_1/a = 0.4$ and remains distant from the nodal line. The behavior of the plate vibration of the (0,0) mode is only slightly influenced by varying the excitation position radially because this mode does not have a nodal line and a circle. Therefore, $r_1/a = 0.4$ is used for comparison with the case of the (1,0) mode. On the other hand, a point force is applied to plate 1 at $r_1/a = 0.2$ in the case of the (0,1) mode, so that the excitation position remains distant from the nodal circle of the (0,1) mode. However, point force F_1 is set to 1 N in all modes. The resonance frequency of the cylindrical sound field is represented by f_{npq} [i.e., the natural frequency corresponding to the (n,p,q) mode].

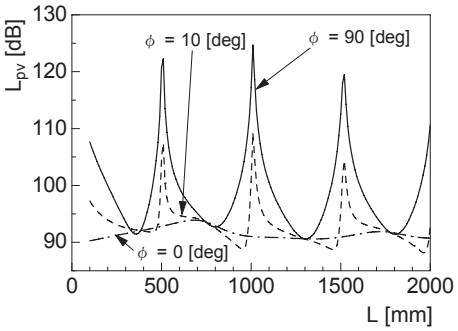

Fig. 2 Variation in sound pressure level with cylinder length in the (0,0) mode

Figure 2 shows the variations in the sound pressure level L_{pv} averaged over the entire sound field when the plate for which $a = 150$ mm and $h = 3$ mm, the R_n of which is 10^8 (i.e., the clamped support), is excited by the natural frequency of $f_{00} = 340$ Hz and the cylinder length L is varied between 100 and 2000 mm. As mentioned in the previous section, the phase ϕ_1 of the plate 1 vibration is fixed as 0 deg, whereas the phase ϕ_2 of the plate 2 vibration is set to 0, 10, or 90 deg. These phases are related by the phase difference ϕ as follows:

$$\phi = \phi_2 - \phi_1 . \tag{9}$$

The sound pressure level L_{pv} varies only slightly over the entire range of L when $\phi = 0$ deg but varies substantially and exhibits peaks in the vicinity of $L = 510$, 1010, and 1520 mm when $\phi = 10$ and 90 deg. The value of L_{pv} is lower when $\phi = 10$ and 90 deg and is almost identical at all phase differences near $L = 380$, 750, 1290, and 1770 mm. The

acoustic modes that cause L_{pv} to have peaks at L = 510, 1010, and 1520 mm are conjectured to be (0,0,q) modes because both plates vibrate in the (0,0) mode.

The vibration of plate 2 has a significant effect on the formation of the sound field and vibroacoustic coupling, despite not being driven by a harmonic point force, whereas the influence of ϕ on the acoustic characteristics has only been described for ϕ = 0, 10, and 90 deg. Figure 3 shows the variation in L_{pv} when ϕ ranges from 0 to 180 deg. In order to clearly indicate changes in L_{pv} with respect to L, the range of L is selected to be between 830 and 1010 mm because minimum and maximum values, respectively, of L_{pv} are near these lengths when ϕ = 90 deg, as shown in Fig. 2. Note that L_{pv} exhibits minimum and maximum values in the vicinity of ϕ = 40 and 130 deg, respectively, at L = 830 mm. These minimum and maximum values shift to lower ϕ as L increases, and the maximum value of L_{pv} increases as ϕ decreases. When L = 1010 mm, the maximum value of L_{pv} appears in the vicinity of ϕ = 90 deg, whereas the minimum value of L_{pv} disappears from the range of ϕ. This change in L_{pv} with ϕ indicates that the acoustic characteristics depend strongly on the vibration of plate 2, i.e., there are ranges of ϕ that intensify or suppress coupling between the plate vibrations and the sound field. The values of ϕ at which L_{pv} is a maximum are denoted by ϕ_{max}.

3.2 *Phase difference that maximizes the sound pressure level*

Figure 4(a) shows the variations in ϕ_{max} for both the (0,0) and (1,0) modes in order to clarify the difference between these two vibration modes, and the values of ϕ_{max} that maximize L_{pv} are plotted by circles. For the (0,0) mode, ϕ_{max} is approximately 83 deg at L = 100 mm and decreases gradually with increasing L up to approximately L = 380 mm, where ϕ_{max} suddenly increases to over 90 deg and then decreases with increasing L again. This behavior of ϕ_{max} is repeated in a similar manner as L increases to L = 2000 mm. The abrupt changes in ϕ_{max} are centered at approximately 90 deg. When plate 1 vibrates in the (1,0) mode, for which f_{10} is 710 Hz, although the rapid changes in ϕ_{max} differ from those of the (0,0) mode in L, ϕ_{max} behaves in a similar manner to that in the (0,0) mode. Figure 4(b) shows the variations in L_{pv} corresponding to the variation in ϕ_{max} with L. Here, L_{pv} corresponding to ϕ_{max} has maxima as ϕ_{max} is approximately 90 deg and is denoted by the circles in Fig. 4(a). Peaks in L_{pv} indicate that vibroacoustic coupling between the plate vibrations and the sound field is promoted. Note that f_{nm} and f_{npq} must be approximately equal for peaks in L_{pv} to appear.

Figures 5(a) and 5(b), respectively, show plots of ϕ_{max} and L_{pv} for the plates of h = 3 mm and $R_n = 10^8$ with a = 100 and 200 mm that vibrate in the (1,0) mode, for which f_{10} is 1595 and 400 Hz, respectively. The periods of ϕ_{max} and the peaks of L_{pv} at a = 100 mm become shorter than those at a = 150 mm because the natural frequency increases with decreasing a. However, when a = 200 mm, the behaviors of ϕ_{max} and L_{pv}, being non-periodic, differ significantly from the above results. Note that ϕ_{max} remains almost constant in the vicinity of 90 deg and decreases abruptly around L = 430, 860, 1290, and 1720 mm. In contrast, L_{pv} tends to decrease in a steadier fashion with increasing L and has extremely small peaks when ϕ_{max} decreases abruptly. The plate vibration of the (1,0) mode is also coupled to the sound field of the (1,1,q) modes due to their similarity to the acoustic mode. Consequently, each acoustic mode exhibits peaks in L_{pv} with

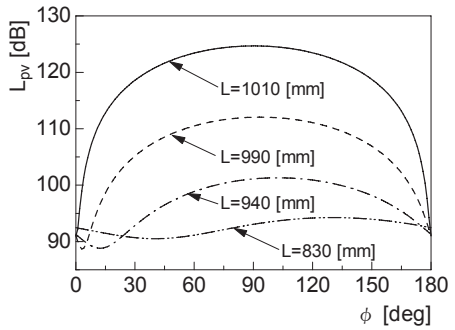

Fig. 3 Variation in sound pressure level with phase difference in the (0,0) mode

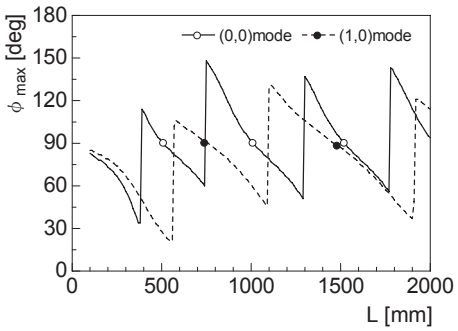

(a) Phase difference

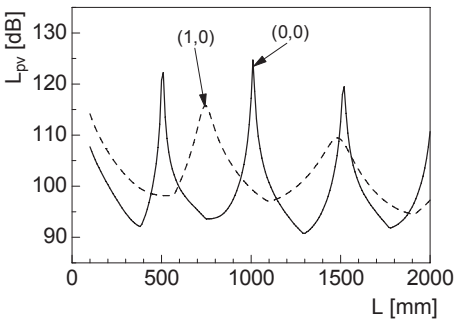

(b) Sound pressure level

Fig. 4 Variations in phase difference and sound pressure level with cylinder length in the (0,0) and (1,0) modes

strong coupling with the respective vibration modes, when the natural frequency f_{10} of the vibration mode coincides with the resonance frequency f_{11q} of the corresponding acoustic mode at a = 100 and 150 mm. However, for the case in which a = 200 mm for the (1,0) mode, f_{10} never reaches f_{11q} over the entire range of L and decreases with increasing a, so that ϕ_{max} does not exhibit abrupt changes, which indicate shifts in q of the (1,1,q) mode, and L_{pv} does not peak decidedly, as in the other cases, because coupling between (1,0) and (1,1,q) modes is suppressed due to the relationship between f_{10} and f_{11q}. In contrast with the (1,1,q) modes, the (0,0,q) modes give rise to peaks in L_{pv}, but these peaks are very small due to the significant difference between the (1,0) and (0,0,q) modes in modal shapes.

Figures 6(a) and 6(b), respectively, show ϕ_{max} and L_{pv} as functions of L for the plate with a = 150 mm, h = 3 mm, and R_n = 10^8, which vibrates in the (0,1) mode. Note that ϕ_{max} varies with a short period and behaves in a more complicated manner as compared to the other cases. In contrast, L_{pv} has peaks at intervals of approximately 130 mm and has more peaks over the entire range of L than other cases, even though f_{01} = 1325 Hz, which never reaches f_{01q} over the entire range of L. The peaks are caused by the (0,0,q) modes, the resonance frequencies of which are equal to f_{01}, because, like the (0,0) mode, the (0,1) mode, being distinct from the two-dimensional (0,0,q) modes in a lateral cross-sectional plane of the cavity in the radial order, is symmetric about the z-axis. The (0,0,q) modes are the dominant modes for all values of L.

3.3 *Parametric study of conditions to enhance vibroacoustic coupling*

In order to clarify the geometric conditions under which vibroacoustic coupling is promoted, the geometric parameters L_{qh} and a_h are defined. When the natural frequency f_{nm} is coincident with the resonance frequency f_{npq}, i.e., L_{pv} peaks, as shown in the previous section, L_{qh} is the length L divided by the longitudinal order q and the thickness h, and a_h is the ratio of the radius a to h.

Figure 7(a) shows the relationship between L_{qh} and a_h for the (0,0), (1,0), and (0,1) modes when R_n = 10^8. The lines for the (0,0), (1,0), and (0,1) modes are plotted based on f_{00q}, f_{11q}, and f_{01q} respectively, the acoustic modes of which have similar modal shapes to their vibration modes. The figure also shows the lines for the (1,0) and (0,1) modes based on f_{00q} due to coupling with (0,0,q) modes. L_{qh} tends to increase with a_h. In particular, L_{qh} based on f_{00q} is linear over the entire range of a_h. On the other hand, when a_h is varied in the proximity of each L_{qh} based on f_{00q} in the range of small a_h, L_{qh} based

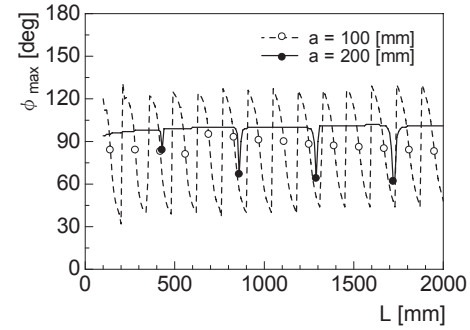

(a) Phase difference

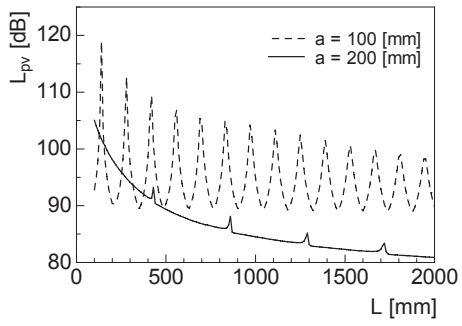

(b) Sound pressure level

Fig. 5 Variations in phase difference and sound pressure level with cylinder length in the (1,0) mode when plate radius changes

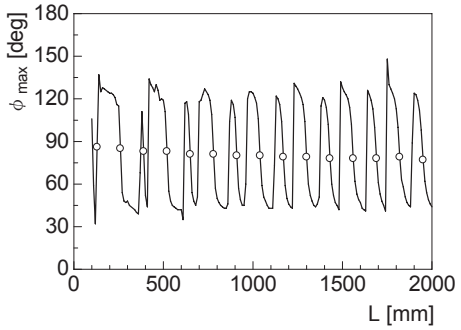

(a) Phase difference

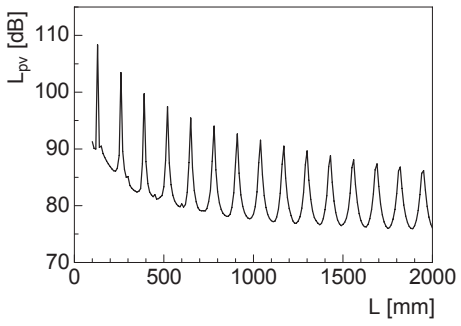

(b) Sound pressure level

Fig. 6 Variations in phase difference and sound pressure level with cylinder length in the (0,1) mode

on f_{11q} and f_{01q} have higher rates of increase than L_{qh} based on f_{00q} and the difference between these L_{qh} increases gradually with increasing a_h. The difference between L_{qh} based on f_{11q} and f_{01q} and L_{qh} based on f_{00q} continues to increase up to a_h = 52 and 47, respectively, and L_{qh} based on f_{11q} and f_{01q} does not exist beyond these points. Figure 7(b) shows the relationship between L_{qh} and a_h when $R_n = 10$. The changes in L_{qh} with a_h are similar to those for $R_n = 10^8$, whereas the variation of L_{qh} with a_h differs from that of $R_n = 10^8$ when L_{qh} vanishes.

As described above, the condition for enhancing vibroacoustic coupling and for maximizing the sound pressure level can be determined from a_h and L_{qh} according to their variation with the vibration mode and the support conditions of the plate. Applied to design of the new electricity generation system, the results reveal that the (0,0) and (0,1) modes can cover a wide range of a_h. However, in the (0,1) mode, the (0,0,q) mode is excited as the dominant acoustic mode for almost all a_h, because the (0,0,q) mode is similar to the (0,1) mode from the viewpoint of the symmetry about the z-axis, and the natural frequency of the (0,1) mode can reach its resonance frequency, which is always lower than the natural frequency of the (0,1,q) mode. On the other hand, in the (1,0) mode, the application is limited by a_h, because the (1,1,q) mode that promotes coupling is extremely suppressed under the condition that f_{10} cannot reach f_{11q}.

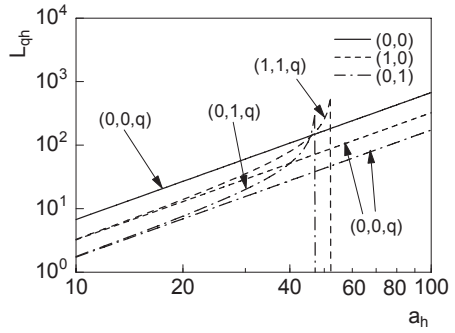

(a) $R_n = 10^8$

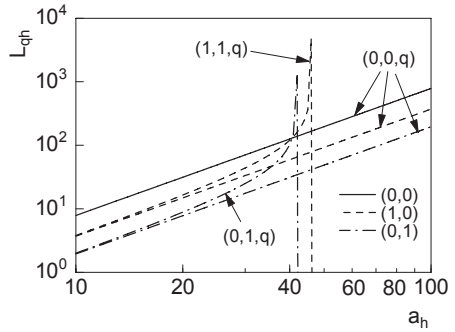

(b) $R_n = 10$

Fig. 7 Conditions by which to maximize the sound pressure level in expressions involving the terms L_{qh} and a_h

4. Experiment

4.1 *Experimental apparatus and method*

Figure 8 shows the experimental apparatus used in the present study. The cylindrical structure consists of a steel cylinder with circular aluminum end plates that are 3 mm thick. The cylinder has inner radius of 153 mm, and these lengths can be varied from 200 to 2000 mm in order to emulate the analytical model. A harmonic point force excites only one end plate. This force is applied to the plate by a small vibrator, the amplitude of which is controlled to be 1 N. The excitation frequencies f_e are the natural frequencies f_{nm} obtained from the experimental modal analysis. The position of the point force r_1 is normalized by radius a, and the (0,0), (1,0), and (0,1) modes are used in this investigation. The position of the point force is set to $r_1/a = 0.4$ for the (0,0) and (1,0) modes and to $r_1/a = 0.2$ for the (0,1) mode in order to avoid the nodal circle. In the present study, the main characteristic of the plate vibration under consideration is the phase difference between the plate vibrations. Therefore, acceleration sensors are installed on both plates to measure this phase difference. In order to estimate the internal acoustic characteristics, the sound pressure level in the cavity is measured by using a condenser microphone with a probe tube, the tip of which is located in the vicinity of the non-excited plate and the cylinder wall, which is the approximate location of the maximum sound pressure level.

4.2 *Experimental results and discussion*

Figure 9(a) shows the variations in the theoretical and experimental phase differences between the vibrations of the two plates as a function of cylinder length L. The excitation frequency f_e is set to 280 Hz in order to induce the (0,0) mode for a plate in this analysis. The experimental value of f_e is 282 Hz. In the theoretical results, only ϕ_{max}, at which the

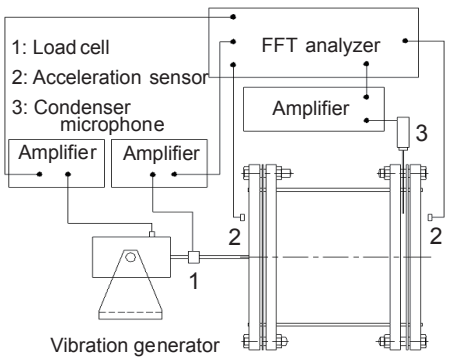

Fig. 8 Configuration of the experimental apparatus

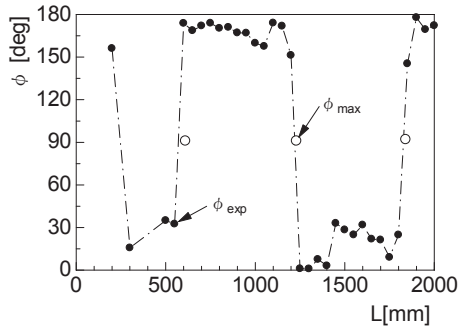

(a) Phase difference

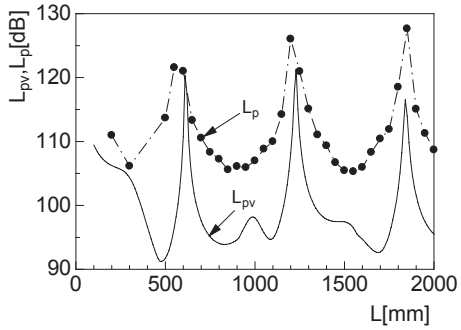

(b) Sound pressure level

Fig. 9 Comparison between theoretical and experimental results for phase difference and sound pressure level in the (0,0) mode

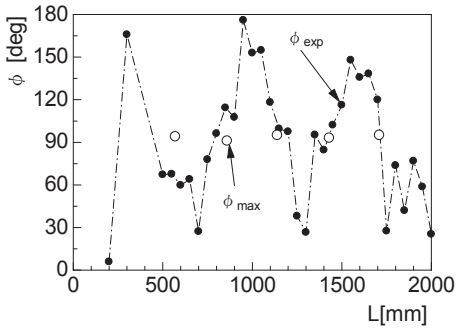

(a) Phase difference

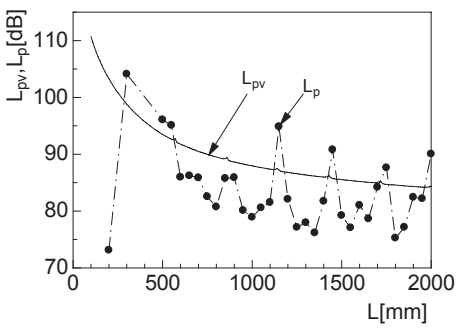

(b) Sound pressure level

Fig. 10 Comparison between theoretical and experimental results for phase difference and sound pressure level in the (1,0) mode

sound pressure level L_{pv} averaged over the entire sound field peaks, is plotted in order to indicate the amplification of the sound pressure level. The theoretical results for ϕ_{max} differ from those for a = 150 mm in Fig. 4(a), in which the intervals between the values of L for the above ϕ_{max} are shortened, because the natural frequency decreases with the decrease in R_n. In the experimental results, the value of ϕ_{exp} remains approximately constant at 180 deg when L is extended from 550 to 1150 mm, but falls rapidly to approximately 0 deg and remains close to 0 deg for values of L up to 1750 mm. Beyond L = 1750 mm, ϕ_{exp} again increases rapidly to approximately 180 deg. The phase difference then remains almost constant up to L = 2000 mm. Figure 9(b) shows the variations in L_{pv}, corresponding to ϕ_{max} in the analysis, and in the sound pressure level L_p measured in the experiment. Peaks in L_{pv} for ϕ_{max} appear at L = 610, 1230, and 1840 mm, at which ϕ_{max} is approximately 90 deg. These peaks are caused by the (0,0,1), (0,0,2), and (0,0,3) modes, respectively. Here, L_p increases significantly at 550, 1200, and 1850 mm. In addition, ϕ_{exp} exhibits rapid changes around these values of L, and the ϕ_{max} appears at the midpoints of the rapid changes in ϕ_{exp}.

Figures 10(a) and 10(b) show the theoretical and experimental results for the phase difference and sound pressure level for the (1,0) mode when a plate is excited at f_e = 600 Hz. Figure 10(a) shows the variations in ϕ_{max} and ϕ_{exp}, and Fig. 10(b) shows the variations in L_{pv} and L_p with L. In this case, f_e does not reach f_{11q} because a_h is greater than 50 [see Fig. 7(b)], so that the (1,0) mode is poorly coupled with the(1,1,q) modes. Since the (1,0) mode is coupled to the (0,0,q) modes that differ from the two-dimensional modes, ϕ_{max} is approximately 90 deg in the vicinity of L = 850, 1150, 1450, and 1750 mm. The experimentally measured ϕ_{exp} varies frequently between 0 deg and 180 deg. Being somewhat erratic, these changes are gradual in comparison with those of the (0,0) mode. Therefore, L_{pv} does not have peaks like those for the (0,0) mode, and L_{pv} decreases monotonically with increasing L, as in the case for a = 200 mm, as shown in Fig. 5(b). In addition, L_{pv} has extremely small peaks in the vicinity of the above values of L. In contrast, although L_p tends to decrease with increasing L in a similar manner to L_{pv}, the peaks in L_p are clearer than the peaks in L_{pv} in the vicinity of the above values of L. Moreover, ϕ_{exp} approaches 90 deg when L_{pv} and L_p peak at the above values of L, so that the behavior of ϕ_{exp} associated with the maximum sound pressure level is similar to that of the (0,0) mode.

In order to theoretically and experimentally investigate the (0,1) mode, when a point force of f_e = 1135 Hz is applied to a plate, Fig. 11(a) shows the variations in ϕ_{max} and ϕ_{exp} with L and Fig. 11(b) shows the variations in L_{pv} and L_p with L. In this case, f_e never reaches f_{01q} because a_h is greater than 50 [see Fig. 7(b)], so that the (0,1) mode is coupled with the (0,0,q) modes instead of with the (0,1,q) modes. Since both the (0,1) and (0,0,q) modes are symmetric about the z-axis, even though these modes do not coincide on the radial order m, ϕ_{max} appears at the interval of the (0,0,q) mode due to coupling between these modes. Note that ϕ_{exp} varies through the circles of ϕ_{max} in the vicinity of 90 deg in a somewhat erratic manner. These results are based on relatively rough measurements, as compared to the measurements for the other modes, due to shortening of the periodic intervals. However, both L_{pv} and L_p have peaks in the vicinity of 90 deg, around which ϕ_{exp} approaches ϕ_{max}.

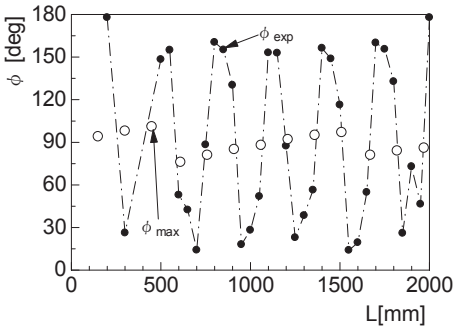

(a) Phase difference

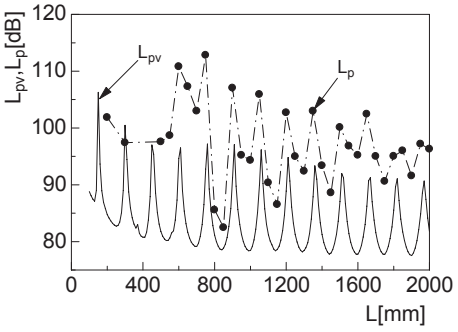

(b) Sound pressure level

Fig. 11 Comparison between theoretical and experimental results for phase difference and sound pressure level in the (0,1) mode

5. Conclusion

In order to apply the acoustic energy to the new electricity generation system, vibroacoustic coupling between plate vibrations and a sound field is investigated for a cylindrical structure with circular end plates. Only one end plate is excited by a harmonic point force, the frequency of which is the natural frequency of each plate. Vibroacoustic coupling is estimated for different radii, thicknesses, and support conditions of the plate. The present study focused on the phase difference between the vibrations of the two plates in order to promote coupling and to maximize the sound pressure level.

The theoretical investigation revealed that if the natural frequency reaches the resonance frequency, the two-dimensional mode of which has a similar modal shape to the vibration mode, the sound pressure level is maximized when the phase difference is close to 90 deg. By using the cylinder length and the radius and thickness of the plates as geometric parameters, the relationships between the parameters can be completely normalized for each vibration mode and each support condition, enabling the dimensions that maximize the sound pressure level via vibroacoustic coupling to be predicted. The experiment results demonstrate that the theoretical estimation is justified via changing the cylindrical length and vibration modes, so that the theoretical results are regarded as a significant reference for the design of a new electricity generation system.

6. References

1) Hayamizu, K. : Device for electric generation, Japanese Patent Disclosure 2010-200607 (2010).
2) Hayamizu, K., Ando,R. and Takefuji,Y. : Simultaneous providing device of baseband and carrier signal using sound-generated electricity, Mobile Multimedia Communications, No.105-80 (2005-5), pp.47-49.
3) Cheng, L. and Nicolas, J. : Radiation of sound into a cylindrical enclosure from a point-driven end plate with general boundary conditions, Journal of the Acoustical Society of America, Vol.91, No.3 (1992), pp.1504-1513.
4) Cheng, L. : Fluid-structural coupling of a plate-ended cylindrical shell: vibration and internal sound field, Journal of Sound and Vibration. Vol.174, No.5 (1994), pp.641-654.
5) Moriyama, H. : Modal characteristics of sound field in cylindrical enclosure with end plates supported by elastic surround, The Journal of the Acoustical Society of Japan, Vol.58, No.6 (2002), pp.338-345.